

Article

Early Warning and Joint Regulation of Water Quantity and Quality in the Daqing River Basin

Liang Chen ^{1,2,*}, Mingxiang Yang ^{1,2,*}, Yang Liu ³ and Linjiang Nan ⁴¹ China Institute of Water Resources and Hydropower Research, Beijing 100038, China² State Key Laboratory of Simulation and Regulation of Water Cycle in River Basin, Beijing 100038, China³ School of Civil Engineering, Tianjin University, Tianjin 300350, China⁴ College of Water Resource & Hydropower, Sichuan University, Chengdu 610065, China

* Correspondence: chenliang@iwhr.com (L.C.); yangmx@iwhr.com (M.Y.)

Abstract: In the recent decades, the issue of water-resource security of the Daqing River Basin, which is one of the five major rivers in the Haihe River Basin, has become increasingly serious affected by climate change and human activities. In this paper, a dynamic simulation and early warning model of water quantity and quality in this basin based on the SWAT model was constructed to promote the implementation of water environment quality and safety bottom line in the Beijing-Tianjin-Hebei region. The results of the study are as follows: (1) When encountering a once-in-a-century rainstorm, the flood pressure of Zijingguan in the flood season is the highest, with the highest water level reaching 521.23 m, and the overall maximum runoff follows the order of Zijingguan > Fuping > Zhangfang. (2) When the NH₃-N emissions are reduced by 37.64~85.10% in each month (based on the level in 2017), the water quality at the outlet of the basin can reach the standard, and the upper limit of NH₃-N emissions is 504.5 t/m. (3) The regulation and control scheme seeking to “ensure the base flow with standard water quality” and “optimize NH₃-N annual emission” is proposed in this paper. The NH₃-N concentration at the outlet of all watersheds can reach the standard when the basic runoff of each sub-basin reaches 0.01 to 10.32 m³/s. In addition, concentrating the emission in July, August, and September and reducing the emission intensity of NH₃-N in proportion can significantly reduce the monthly average NH₃-N concentration (<1.99 mg/L) at the outlet section of the basin.

Keywords: water quantity; water quality; early warning; joint regulation; Daqing River

Citation: Chen, L.; Yang, M.; Liu, Y.; Nan, L. Early Warning and Joint Regulation of Water Quantity and Quality in the Daqing River Basin. *Water* **2022**, *14*, 3068. <https://doi.org/10.3390/w14193068>

Academic Editors: Xiaosheng Qin and Yurui Fan

Received: 31 August 2022

Accepted: 23 September 2022

Published: 29 September 2022

Publisher's Note: MDPI stays neutral with regard to jurisdictional claims in published maps and institutional affiliations.



Copyright: © 2022 by the authors. Licensee MDPI, Basel, Switzerland. This article is an open access article distributed under the terms and conditions of the Creative Commons Attribution (CC BY) license (<https://creativecommons.org/licenses/by/4.0/>).

1. Introduction

The Daqing River is one of the five major rivers in the Haihe River Basin and an important water system in the Beijing-Tianjin-Hebei region [1]. The Xiong'an New Area is also located in the hinterland of the Daqing River Basin. The national strategy for “Integrated Development of Beijing-Tianjin-Hebei”, which was launched in 2014, further promoted the position of the Daqing River Basin in China's major strategy. In recent decades, as a sensitive area affected by climate change and human activities [2], the climate and environmental conditions of the Daqing River Basin have undergone tremendous changes, and the issue of water resources security in the basin has become increasingly serious.

The river basin, as a type of freshwater resource, is generally put in a state of jeopardy in terms of quantity and quality due to the development in industry, agriculture, and urbanization. The quality of surface water in river basins plays a key role in water-resource security. So, measuring water quality, which is of high importance in water-resource management, is normally carried out in disparate ways. In this way, an accurate estimation of WQI (Water Quality Index) is one of the most challenging issues in the water-quality studies of surface-water resources [3,4]. Due to the intrinsic limitations of conventional models, Data-Driven Models (DDMs) have been frequently employed to assess the WQI for natural streams [5]. The DDMs-based WQI formulation is used to assess river in in

the reliability-based probabilistic framework to consider the effect of any uncertainty and randomness in the input parameters. In addition, multiple-kernel support vector regression (MKSVR) algorithm was also proposed to estimate the hard-to-measure parameters from those that can be measured easily [6–9]. For solving the optimization problem of the MKSVR, the particle swarm optimization (PSO) algorithm was used.

With the increasing complexity of global water-resources problem [10,11], The single study of water resources' allocation has gradually changed to a field of sustainable utilization of water resources which comprehensively considers water-quality constraints, water environmental pressures, etc. [12,13]. The principles and methods of water-resource-optimization management have been normally proposed by linear decision-making, multi-objective planning, and multi-level management [14,15]. On this basis, the joint application of multi-objective and multistage water resources' optimal management has further been put forward [16,17], so as to realize the optimal regulation and allocation of water resources. With the development of complexity analysis and simulation optimization technologies, model simulation has become one of the important means of regulation and control of water resources [18].

At the watershed scale, numerous simulations and predictions research studies regarding the watershed hydrological process have been performed based on hydrological models and global climate change [19–21]. The rationality and effectiveness of water resources' allocation has been analyzed to improve the available water resources [22,23]. The SWAT hydrological model with downscaling deviation analysis has been applied to explore the response of runoff change to different climate scenarios [24–28]. Furthermore, the coupled programming model [29–31] has often been used to study the water-resource allocation and system benefits under different water inflow conditions. At the regional scale, the management model of surface water, groundwater, and sewage was established, with the goal of maximizing the benefits, so as to provide the basic data for the regulation of water quantity and quality [32]. By using the stochastic fuzzy neural network model (SFNN model), the indicators of social economy, water quantity, and water quality in regional water resources systems were treated as fuzzy parameters, and the linkage relationship between water quantity and water quality was fully considered, so as to study the sustainable allocation of water resources [33,34]. The dynamic nonlinear programming model was applied to the integrated management of water quality and quantity [35], and the efficiency, fairness, and sustainability of the urban water supply were explored.

Other scholars have adopted the copula joint distribution model for the evaluation of water quality and quantity and proposed measures to strengthen regional pollutant control and treatment [36,37]. A joint probability distribution approach is used to describe relationship between water quality and flow discharge by multiple variables [38]. The copula theory has been widely applied in the field of hydrology and water environment in recent decades, as it can relate different univariate marginal distributions without changing the dependence structure and the initial data information in the transformation process [39,40]. Three copula types are commonly used: Archimedean copulas, which are relatively more convenient for symmetric relationships; Elliptic copulas, which are suitable for symmetric relationships; and Vine copulas, which can combine different copula types in low dimensions [41,42]. These copula functions can be applied to detect the joint change-point of the precipitation–discharge relationship and perform flood-risk analysis [43–46].

Unlike the previous studies on the joint distribution of water quantity and quality, the main novelty of this study is that it explored a new joint regulation scheme of water quantity and quality by developing a dynamic simulation and early warning model in the Daqing River Basin, based on the SWAT model. The water-level elevation and the rainstorm in different recurrence intervals were simulated. The relationship between the pollutant discharge amount and concentration in multiple pollutant discharge and meteorological scenes were further analyzed. These two major steps are involved in the detection of early warning values of water quantity and pollutant discharge in this basin, and they illustrate a suitable joint regulation scheme, using the proposed method. Therefore, it is of great

significance to carry out joint early warning and regulation research by incorporating both water quantity and quality in the Daqing River Basin, which can serve as a useful and reliable tool for an impartial diagnosis and management of water resources. It will further promote the implementation of the three red lines of “water resources utilization upper line, ecological space protection red line and water environment quality and safety bottom line” in the Beijing-Tianjin-Hebei region [47].

2. Materials and Methods

2.1. Study Area

The Daqing River Basin is located in the middle of the Haihe River Basin on the North China Plain (113°40′ E–117°00′ E, 38° N–40° N) and has a total basin area of 43,060 km², with the annual precipitation of 727 mm and annual runoff of 60.2 m³/s (Figure 1). Rainfall in the basin is unevenly distributed throughout the year, mostly occurring in the form of rainstorms, mainly falling from July to August, a period that accounts for more than 70% of the annual rainfall. During the flood season, due to the influence of cold and warm air flow and subtropical high, heavy rain forms easily, especially in the Fuping–Zijingguan area. The annual average temperature in the basin is 12.4 °C, and the average annual evaporation is 1309 mm. Soil types are divided into 16 categories and 36 subclasses—mainly cinnamon soil. Cultivated land accounts for 52.4%, followed by woodland, grassland, and construction land. The water pollution in the Daqing River Basin is complex and diverse, and the pollution mainly originates from domestic sewage discharge, pesticide and fertilizer application, and factory sewage discharge, with the standard rate of the river being lower than 30%.

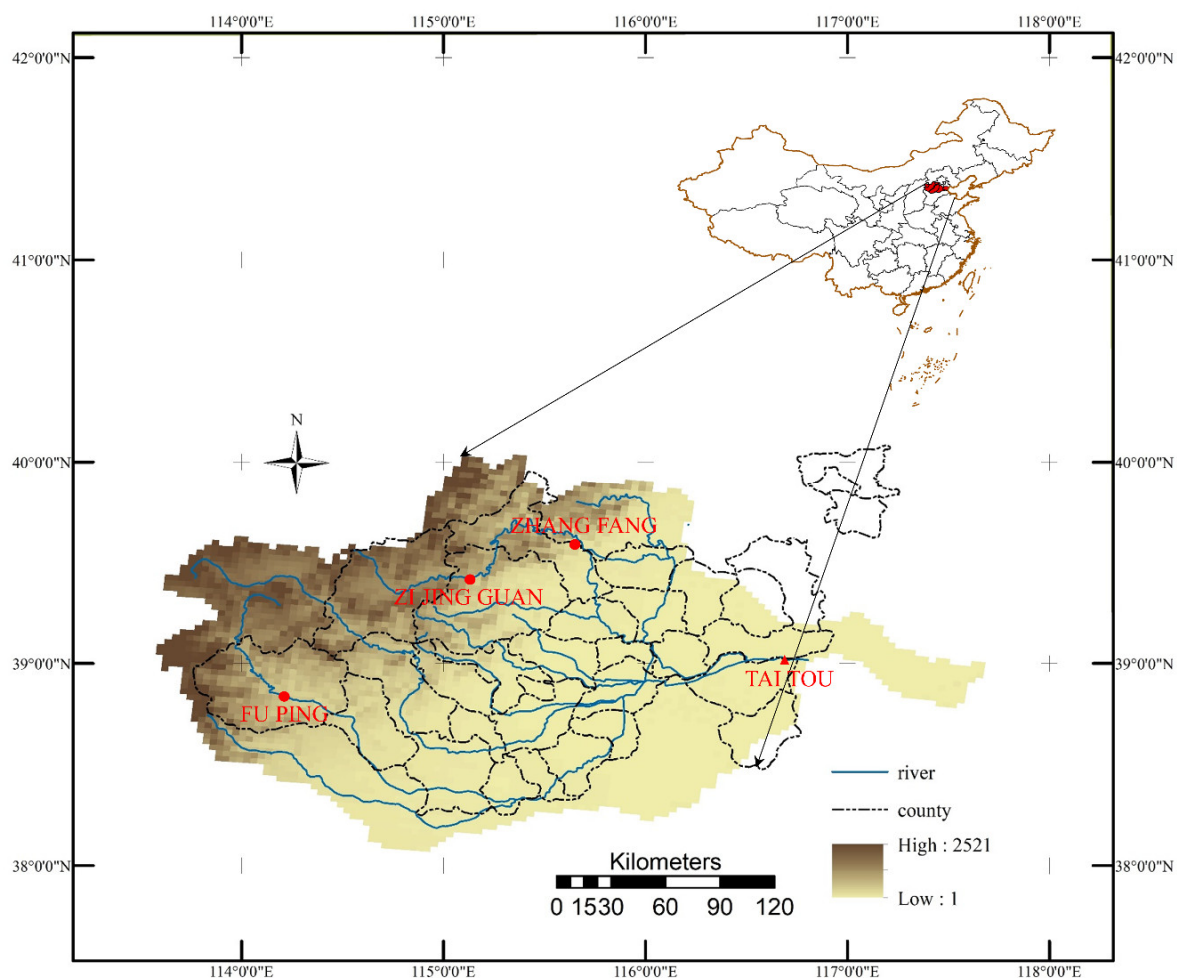


Figure 1. Schematic diagram of the location of the Daqing River Basin.

2.2. Data Materials

The data covered in this study mainly include DEM, land use, soil type, meteorology, hydrology, and pollution (Table 1).

Table 1. Data sources and treatment.

Data Types	Initial Source Data	Processing Suitable to the Model/Study	
		Processing	Data Display
Basic data for SWAT	DEM	ASTER GDEM V3	\
	Land use	Remote sensing monitoring data of land use status in China in 2010	Reclassification, land-use grid data, land-use index table
	Soil type	Harmonized World Soil Database (HWSD), China Soil Data Set (v1.1)	Soil-distribution grid file, soil parameter database, soil-type index table
	Meteorology	Daily scale data of National Meteorological Data Service Center (v3.0)	Weather generator parameters (R language programming calculation)
Data required for research	Hydrology	Hydrologic yearbook of the Haihe River Basin	Daily scale data of precipitation, temperature, wind speed, relative humidity, and sunshine intensity from 1 January 2011 to 31 December 2017
	Pollutant discharge	Statistics related to pollutant discharge in the Daqing River Basin	Monthly average flow of each station in the Daqing River Basin from 2006 to 2016
			Monthly scale data in the Daqing River Basin from 2010 to 2017

2.3. Method

In this study, the dynamic simulation model of water quantity and quality in the Daqing River Basin was constructed by using ArcSWAT2012, and its parameters were calibrated and verified. Next, the relationship curve of runoff and water level in the Daqing River Basin was established, and the variation law of runoff and water-level elevation in different recurrence intervals was analyzed by simulating the rainstorm in recurrence intervals, so as to realize the early warning of water quantity in the basin. The relationship between the pollutant discharge (point source and nonpoint source) amount and concentration in a river in multiple-pollutant discharge and meteorological scenes was analyzed, and the early warning value of pollutant discharge was proposed, so as to realize the early warning of water quality. On this basis, a joint regulation scheme of water quantity and quality by which to ensure the river-water quality was put forward. The schematic diagram of the model is shown in Figure 2.

For this research, in the model, the Daqing River Basin was divided into 35 sub-basins and 247 hydrological cells. The division of sub-basins is shown in Figure 3. Floods in the Daqing River Basin are mainly caused by rainstorms occurring in the flood season, with the rainstorm centers often appearing in Fuping and Zijingguan. Therefore, three representative hydrologic stations, namely Zhangfang (Sub-basin 4), Zijingguan (Sub-basin 6), and Fuping (Sub-basin 25), were selected in this paper for water-quantity early warning, and Taitou (sub-basin 14) was selected as the representative station of basin outlet for water-quality early warning and joint regulation.

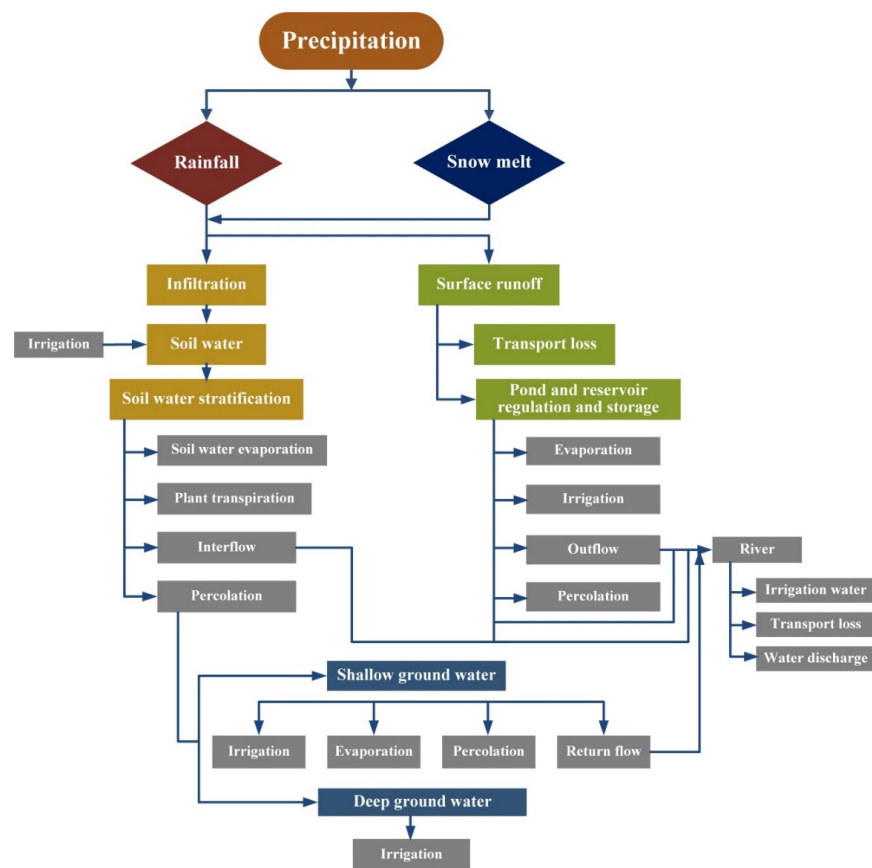


Figure 2. The dynamic simulation model of water quantity and quality in the Daqing River Basin.

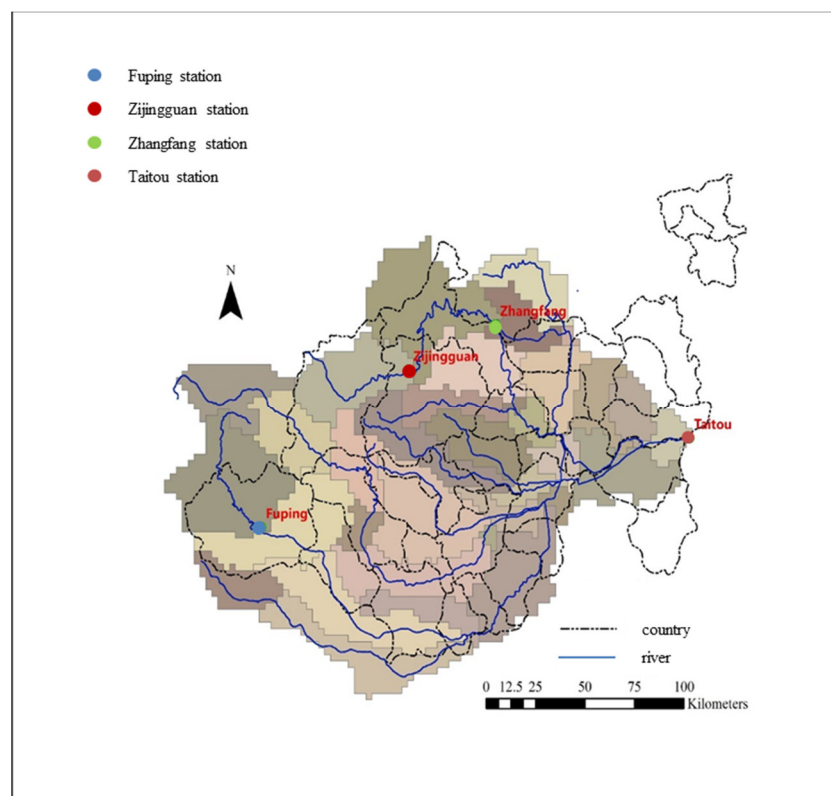


Figure 3. Schematic diagram of sub-basin division in the Daqing River Basin.

3. Results and Discussion

3.1. Model Calibration and Verification

In this study, the runoff parameters were checked by the measured runoff data of Zhangfang, Zijingguan, and Fuping in the Daqing River Basin, and the water-quality parameters were checked by the pollutant amount of the Taitou Station. The calibration period of Zhangfang Station was set as 2006–2010, and the verification period was set as 2011–2013. The calibration period of Zijingguan and Fuping Stations was set as 2006–2012, and the verification period was set as 2013–2016. The calibration period of pollutants at Taitou Station was set as 2013–2014, and the verification period was set as 2015–2016. In this study, the determination coefficient (R^2) [48,49] and Nash–Sutcliffe efficiency coefficient (NSE) [50] were selected to evaluate the simulation effect of the model. The calibration and validation results of the model are shown in Table 2.

Table 2. Calibration and validation results of runoff and water quality in the model.

Stations	Calibration Period		Verification Period	
	R^2	NSE	R^2	NSE
Zhangfang_FLOW	0.61	0.56	0.72	0.52
Zijingguan_FLOW	0.72	0.61	0.88	0.86
Fuping_FLOW	0.76	0.7	0.84	0.72
Taitou_NH ₃ -N	0.66	0.61	0.7	0.69

It can be seen from Table 2 that the monthly simulation results of stations in Zhangfang, Zijingguan, and Fuping are all “satisfactory” ($NSE > 0.5$), while those of NH₃-N at Taitou Station are “very good” ($0.6 < R^2 \leq 0.7$) [51,52]. By comparing and analyzing the simulated and measured values of monthly runoff at three stations, respectively, in Zhangfang, Zijingguan and Fuping (Figure 4), and the simulated and measured values of water quality at Taitou Station (Figure 5), it can be seen that the simulated and observed values have the same trend, the model fitting effect is good, and the model can be used for the further research.

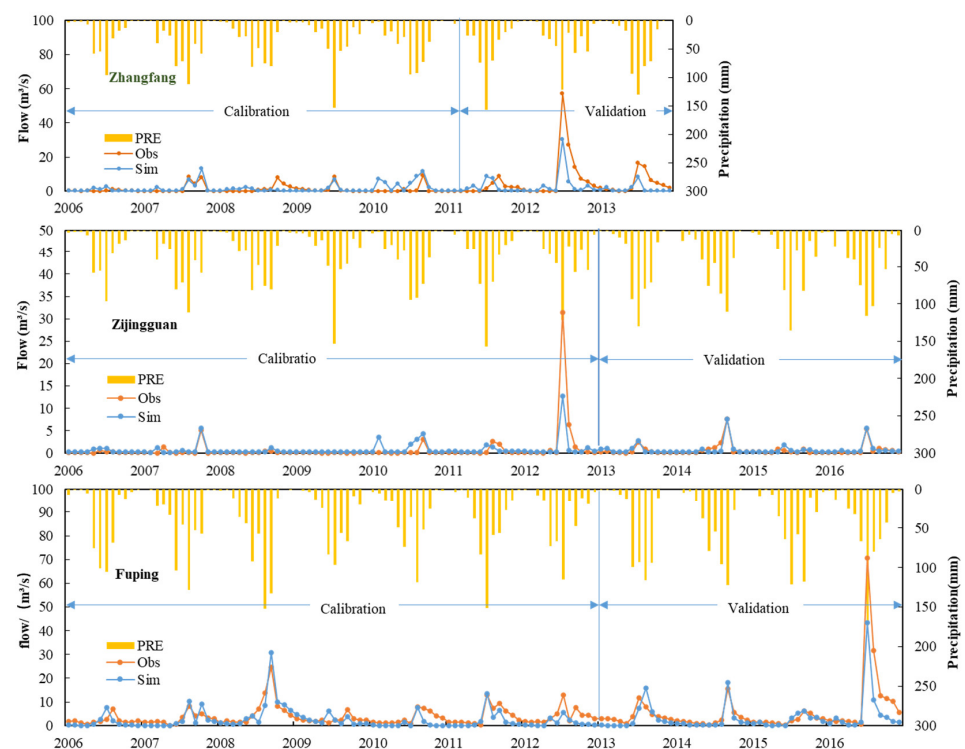


Figure 4. Measured and simulated values of runoff (stations in Zhangfang, Zijingguan, and Fuping).

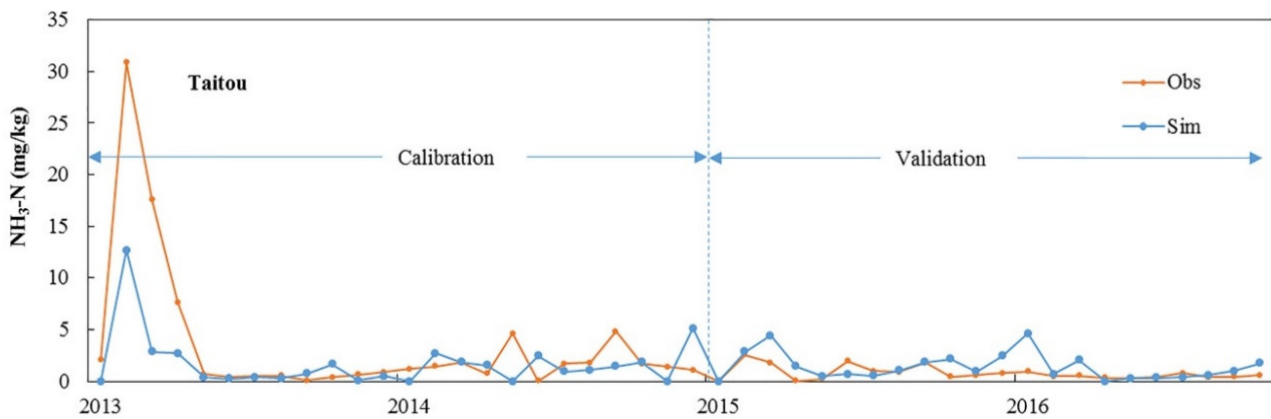


Figure 5. Measured and simulated values of NH₃-N (Taitou Station).

3.2. Water Quantity and Water Quality Early Warning

3.2.1. Water Quantity Early Warning

Due to the fact that Zijingguan and Zhangfang are driven by Yuxian meteorological data, while Fuping County is driven by Lingqiu meteorological data, the data of the Yuxian and Lingqiu meteorological stations were used in this paper as the meteorological data required for scene simulation. By analyzing the measured rainfall data of the Daqing River Basin from 1951 to 2019, the daily rainfall in the recurrence intervals of the Yuxian and Lingqiu meteorological stations was calculated and determined (Table 3), which was taken as the input item of rainfall scene, and the daily average runoffs of Zijingguan, Zhangfang, and Fuping were simulated.

Table 3. Scenes of rainfall recurrence interval.

Rainfall Recurrence Intervals	Maximum Daily in Yuxian (mm)	Maximum Daily Rainfall in Lingqiu (mm)
Once every 5 years	46.38	56.82
Once every 10 years	53.20	65.44
Once every 20 years	62.67	71.78
Once every 50 years	81.43	77.58
Once every 100 years	102.58	80.56

In view of the characteristics of short rainstorm duration and concentrated flood in the Daqing River Basin, the daily average runoff is unable to meet the function of water quantity early warning. In this study, the fitting analysis was further performed regarding the relationship between the daily average runoff and maximum flow and the relationship between water level and flow at three stations, and the results are shown in Figures 6 and 7.

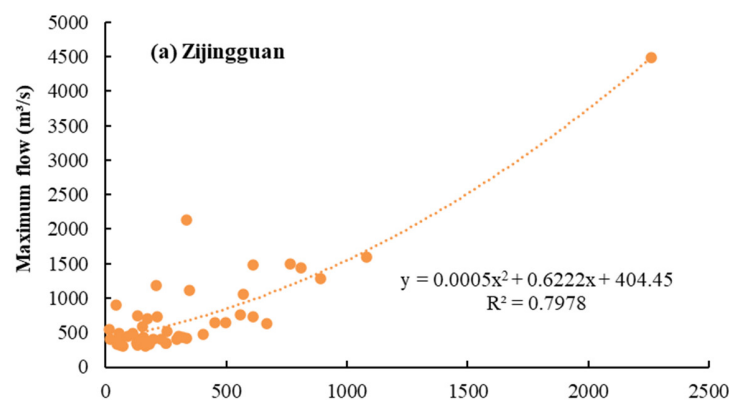


Figure 6. Cont.

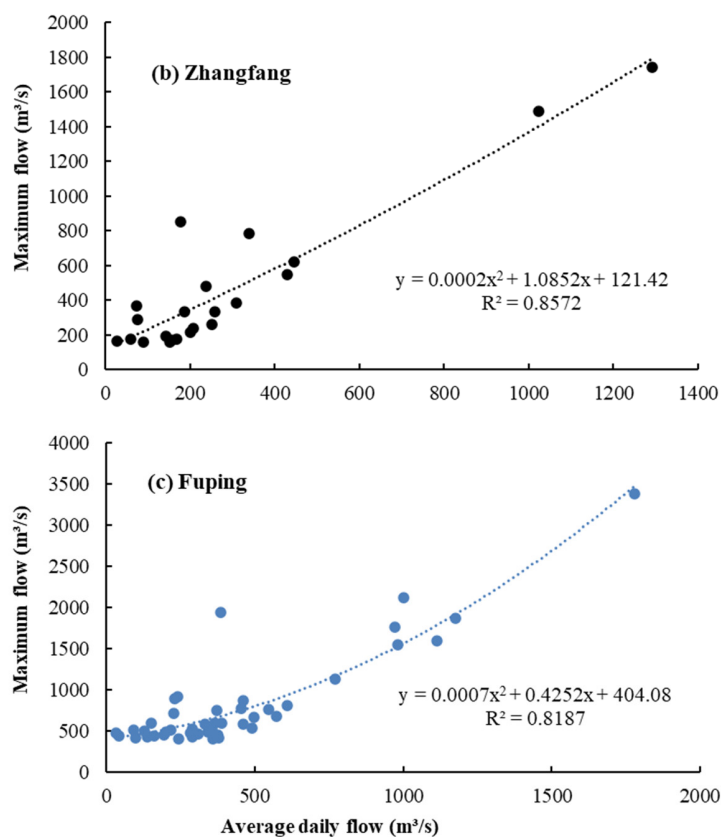


Figure 6. Relationship between daily average flow and maximum flow.

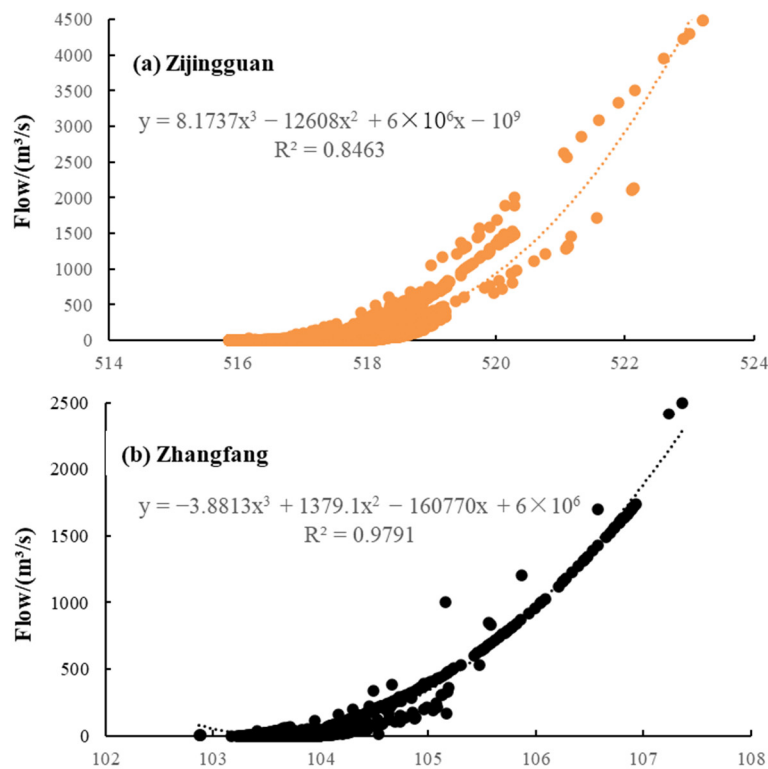


Figure 7. Cont.

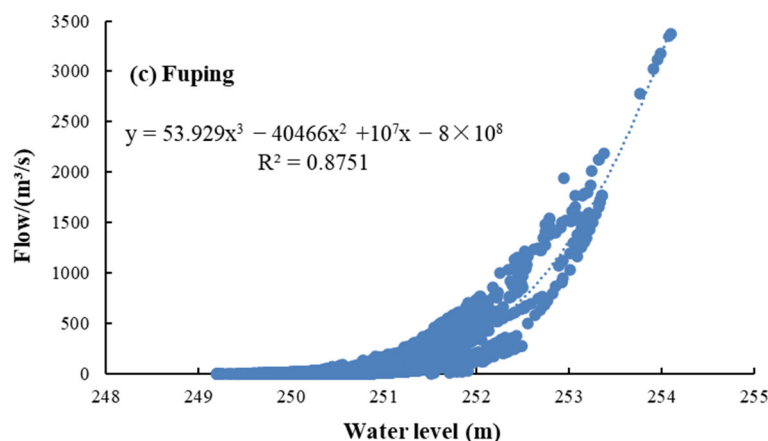


Figure 7. Relationship between water level and flow.

Table 4 shows the response relationship of rainfall, runoff, and water level at Zijingguan, Zhangfang, and Fuping under different rainfall recurrence intervals. It can be seen that, under the same rainfall recurrence interval, there are some differences in the warning values of maximum runoff and maximum water level at different stations. When encountering a once-in-a-century rainstorm, the water level at Zijingguan, Zhangfang, and Fuping reached 521.23 m, 106.12 m, and 253.85 m, respectively, and the flood pressure of Zijingguan during flood season was the highest.

Table 4. Runoff and water-level-warning results of different rainfall recurrence intervals at each station.

Hydrological Stations	Rainfall Recurrence Interval	Rainfall (mm)	Simulated Runoff (m ³ /s)	Calculated Maximum Runoff (m ³ /s)	Calculated Maximum Water Level (m)
Zijingguan	Once every 5 years	46.38	99.8	471.52	519.04
	Once every 10 years	53.20	226.8	571.24	519.25
	Once every 20 years	62.67	571.9	923.82	519.87
	Once every 50 years	81.43	1254.0	1970.95	521.23
	Once every 100 years	102.58	2094.0	3899.75	522.99
Zhangfang	Once every 5 years	46.38	93.21	224.31	104.72
	Once every 10 years	53.20	102	234.19	104.75
	Once every 20 years	62.67	260.6	417.81	105.15
	Once every 50 years	81.43	450.4	650.77	105.55
	Once every 100 years	102.58	762.2	1064.75	106.12
Fuping	Once every 5 years	56.82	579.94	886.10	252.65
	Once every 10 years	65.44	747.01	1112.33	252.85
	Once every 20 years	71.78	834.28	1246.03	252.95
	Once every 50 years	77.58	1133.21	1784.84	253.32
	Once every 100 years	80.56	1582.35	2829.58	253.85

3.2.2. Water-Quality Early Warning

According to the water-quality-monitoring data of Taitou Station from 2015 to 2019, as well as the Environmental Quality Standards for Surface Water (GB3838-2002), the monthly average water quality of Taitou Station for many years was Inferior Class V, and the water quality of all townships in the Daqing River is Class V. The overall water quality is quite poor [53]. NH₃-N, the main pollutant according to monitoring data in long time series, is selected as the control pollutant for early warning of water quality in the Daqing River Basin. According to the Langfang Key Rivers Water Quality Standards Plan (Revised Edition) issued in 2019, the local authorities aim to keep the water quality of the Daqing River Basin stable and for it to remain as Class V water, i.e., the NH₃-N concentration is not to exceed 2 mg/L.

Through the analysis of historical runoff data, 2012, 2017, and 2000 were selected as the representative years of high-, normal-, and low-flow years, respectively. Based on the current year (2017), the point-source discharge was increased or decreased (+50~−50%), and a scene was set every 10%. A total of 33 combined scenes of rainfall and point-source discharges were set (Table 5), so as to simulate the relationship between the emission intensity of pollution sources and the NH₃-N concentration in rivers in different level years (Figure 8).

Table 5. Combined scenarios of rainfall and point-source discharge.

Scenario No.	Rainfall	Intensity of Point-Source Discharge	Scenario No.	Rainfall	Intensity of Point-Source Discharge
1	High-flow years	+50%	19	High-flow years	−10%
2	Normal-flow years	+50%	20	Normal-flow years	−10%
3	Low-flow years	+50%	21	Low-flow years	−10%
4	High-flow years	+40%	22	High-flow years	−20%
5	Normal-flow years	+40%	23	Normal-flow years	−20%
6	Low-flow years	+40%	24	Low-flow years	−20%
7	High-flow years	+30%	25	High-flow years	−30%
8	Normal-flow years	+30%	26	Normal-flow years	−30%
9	Low-flow years	+30%	27	Low-flow years	−30%
10	High-flow years	+20%	28	High-flow years	−40%
11	Normal-flow years	+20%	29	Normal-flow years	−40%
12	Low-flow years	+20%	30	Low-flow years	−40%
13	High-flow years	+10%	31	High-flow years	−50%
14	Normal-flow years	+10%	32	Normal-flow years	−50%
15	Low-flow years	+10%	33	Low-flow years	−50%
16	High-flow years	0			
17	Normal-flow years	0			
18	Low-flow years	0			

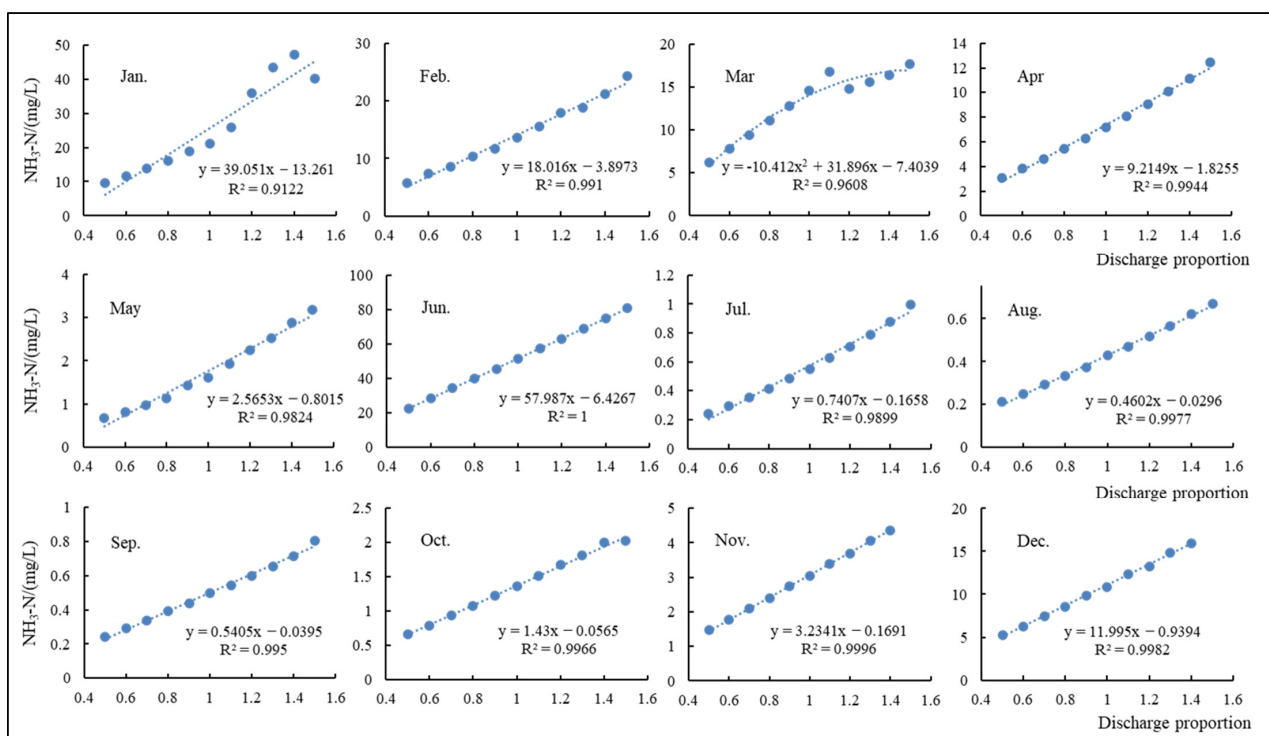


Figure 8. Relationship between the emission intensity of pollution source and NH₃-N concentration in each month (taking the normal-flow year as an example).

The scenario simulation results show that, when the point-source discharge increases by 50% (based on the emissions in 2017), 75% (January–June and October–December), and 75% (January–June and October–December), then the monthly average water quality in both high- and normal-flow years is Inferior Class V. In low-flow years, due to the lower amount of rainfall, some rivers stopped flowing, thereby blocking the movement of pollutants, and 58.3% of the monthly average water quality reached Inferior Class V. When the point-source discharge did not increase, then 58.3% (January, February, March, May, June, November, and December), 58.3% (January, February, March, April, June, November, and December), and 58.3% (January, February, March, April, May, November, and December) of the monthly average water quality reached Inferior Class V in the high-, normal-, and low-flow years, respectively. When the point-source discharge was reduced by 50%, then 41.7% (January, February, March, June, and December), 50% (January, February, March, April, June, and December), and 58.3% (January, February, March, April, May, November, and December) of the monthly average water quality reached Inferior Class V in high-, normal-, and low-flow years, respectively.

Due to the lower amount of natural runoff in the Daqing River Basin, the $\text{NH}_3\text{-N}$ emission is high. For example, when the current discharge is reduced to 50% in a normal-flow year, the monthly average $\text{NH}_3\text{-N}$ concentration still reaches Inferior Class V. However, if the emission is reduced to 85.1%, then the monthly average $\text{NH}_3\text{-N}$ concentration can reach the standard. Therefore, with the aim of reaching the standard of $\text{NH}_3\text{-N}$ concentration at the outlet of the basin (2 mg/L), the early warning values of $\text{NH}_3\text{-N}$ emission in each month and sub-basin in different level years were determined (Table A1 in Appendix A) according to the previous fitting relationship between the emission intensity of pollution sources and $\text{NH}_3\text{-N}$ concentration. The simulation results show that the upper emission limit of July, August, and September in high-, normal-, and low-flow years, respectively, accounted for 68.69%, 68.74%, and 75.05% of the annual emission, while the emission upper limits of July, August, and September in the same level years were significantly higher than those in other months. In addition, for different level years, the upper limit of $\text{NH}_3\text{-N}$ emission was greatly affected by river cutoff, and the total emission amounts in low-flow years were 13.56% and 6.08% higher than those in high- and normal-flow years, respectively.

3.3. Joint Regulation of Water Quantity and Quality

3.3.1. Ensuring the Base Flow with Standard Water Quality

The flow with standard water quality is the lowest flow of the river at which the water quality of the river section must be maintained to meet the local standards [54]. Under the current emission scenario, the monthly average $\text{NH}_3\text{-N}$ concentration in the Daqing River Basin from July to October did not exceed the standard. In these four months, the rainfall was abundant, the river runoff was high, and the river channel's pollutant-holding capacity was relatively large. In other months, the runoff was small, and the river channel's pollutant-holding capacity was poor. Therefore, under the premise of not reducing the discharge, both ensuring a certain river flow and improving the river's pollutant-holding capacity can effectively reduce the river pollution degree [55].

In this paper, the same temperature, relative humidity, wind speed, and sunshine intensity were given, and different daily rainfall scenarios were set to simulate the minimum flow of 35 sub-basins (Table 6). The simulation results show that Sub-basin 5 has the lowest demand for water quality, while Sub-basin 13 has the highest. The $\text{NH}_3\text{-N}$ concentration at the outlet of all watersheds can reach the standard when the basic runoff of each sub-basin reaches 0.01 to 10.32 m^3/s .

Table 6. Minimum flow of guaranteed water quality in sub-basins.

Sub-Basins	Runoff (m ³ /s)	Sub-Basins	Runoff (m ³ /s)
1	0.16	19	4.56
2	1.86	20	5.27
3	1.58	21	4.93
4	1.60	22	0.80
5	0.01	23	6.82
6	0.63	24	0.26
7	1.48	25	5.68
8	2.64	26	2.43
9	0.94	27	1.00
10	1.75	28	3.45
11	3.50	29	0.56
12	6.91	30	2.60
13	10.32	31	0.02
14	4.29	32	6.57
15	0.16	33	1.51
16	1.64	34	4.71
17	8.71	35	0.62
18	2.66		

3.3.2. Optimize NH₃-N Annual Emission

The Daqing River Basin has abundant rainfall, high runoff, a relatively large water environment capacity, and a strong river's pollutant-holding capacity in summer and autumn, while the opposite is true in spring and winter. The reasonable adjustment of the annual discharge of pollutants and optimization measures of discharge intensity based on water environmental capacity can be applied to effectively utilize the river's pollutant-holding capacity in summer and autumn, as well as to ensure that the water quality at the outlet of the basin reaches the standard [55].

Therefore, in this study, on the premise of not increasing the amount of pollutant discharge (based on the emissions in 2017), the warning value of NH₃-N emissions in each month in different level years under the water quality standards was reduced in proportion. In addition, the concentration of NH₃-N after optimized emissions and the maximum and minimum emissions of NH₃-N under the water-quality standards were simulated and calculated according to the optimized emission-intensity and meteorological-data scenarios.

Through simulation (Table 7), taking the high-flow years as an example, the average runoff of the river is the highest in July and August, i.e., 42.57 m³/s and 42.69 m³/s, respectively, and the optimized NH₃-N discharge amount is 3004.87 t and 3118.49 t, respectively. At this time, the discharge intensity of NH₃-N is still able to meet the Class II water standard, which can fully meet the water-quality requirements of the management department. In the normal-flow years, it is found that the water qualification rate of NH₃-N in each sub-basin reached 57.14% in July, August, and September, and the runoff accounts for 57.29% of the total annual runoff. By optimizing the discharge intensity of NH₃-N in the year, the average monthly NH₃-N concentration at the outlet section of the basin was significantly reduced (<1.99 mg/L), and it met the Class V water standard. The simulation results of low-flow years show a similar condition that concentrating the discharge amount in July, August, and September can effectively utilize the river's pollutant-holding capacity, reduce the concentration of pollutants in the river, ensure the river's water quality meets the standard, and promote the ecological improvement surrounding the river, thus proving it to be a strong regulation measure [56–58].

Table 7. Pollutant discharge amount and NH₃-N concentration after optimization.

Month	High-Flow Years			Normal-Flow Years			Low-Flow Years		
	Discharge Amount (t)	Simulated Runoff (m ³ /s)	NH ₃ -N (mg/L)	Discharge Amount (t)	Simulated Runoff (m ³ /s)	NH ₃ -N (mg/L)	Discharge Amount (t)	Simulated Runoff (m ³ /s)	NH ₃ -N (mg/L)
Jan.	0.76	0.21	1.74	96.13	1.47	1.99	5.23	0.70	1.82
Feb.	10.09	0.58	1.01	116.75	0.59	1.94	24.76	3.63	1.94
Mar.	53.53	2.07	1.58	231.81	0.36	1.71	668.90	27.92	1.43
Apr.	787.25	6.98	1.30	290.94	4.85	0.69	1364.47	21.57	1.70
May	565.47	0.59	1.81	765.96	4.51	0.90	851.36	10.11	1.12
Jun.	1212.94	3.73	0.84	104.54	0.35	0.36	532.99	6.02	1.79
Jul.	3004.87	42.57	0.39	2216.67	24.81	0.87	1663.18	2.09	0.77
Aug.	3118.49	42.69	0.34	3093.50	69.98	1.27	2906.43	3.43	0.64
Sep.	1693.75	34.63	0.71	2646.55	89.79	1.36	1840.61	34.42	0.72
Oct.	565.29	17.39	1.81	1008.66	88.24	1.36	667.70	13.47	1.43
Nov.	112.24	15.30	1.41	437.41	28.39	1.51	598.96	12.37	1.59
Dec.	3.85	2.93	1.59	119.62	4.15	1.95	3.96	0.22	1.61

4. Conclusions

Water quantity and quality are two key regulation factors affecting the performance of integrated watershed management. Conventional water-resource assessment and simulation of rivers in the previous literature often dealt with water quantity and quality separately. The nonmonotonic relationship between the water quality and flow discharge of a river, especially in watersheds with significant human activity impacts and high spatiotemporal variations in flows, such as the Daqing River Basin, is often ignored in contrast to near-natural conditions. More specifically, the previous literature on the analysis of water quantity and quality based on copula functions often dealt with the uncertainty analysis of multivariable correlations, risk analysis for water quality, or forecasting of water quality.

The present results indicate that the proposed method can take into account the near-natural law between water quantity and quality to make a more reliable simulation for integrated water resources' management and regulation.

When encountering a once-in-a-century rainstorm, the flood pressure of Zijingguan in the flood season is the highest, with the highest water level reaching 521.23 m, and the overall maximum runoff follows the order of Zijingguan > Fuping > Zhangfang. In addition, when the hydrological station determines the water-level-warning value, the corresponding rainfall can be obtained based on the relationship between rainstorm and water level [59]. Furthermore, when the weather station monitors a certain amount of rainfall, it can also send corresponding water-level-warning information to the hydrological station.

According to the relationship between emission ratio and NH₃-N concentration at the outlet of the basin, when the monthly NH₃-N emissions in different level years were reduced by 37.64–85.10% (based on the emissions in 2017), the water quality at the outlet of the basin could reach the standard, and the upper limit of NH₃-N emissions was 504.5 t/m. The upper emission limits in July, August, and September in high-, normal-, and low-flow years accounted for 68.69%, 68.74%, and 75.05% of the whole year, respectively, and the upper emission limits in July, August, and September in the same level year were significantly higher than those in other months.

In this paper, the regulation-and-control method of basic flow to ensure that the water quality is up to standard was proposed. On the premise of not reducing emissions, we could ensure a certain river flow and improve the river's pollutant-holding capacity. The simulation results showed that the NH₃-N concentration at the outlet of all watersheds could reach the standard when the basic runoff of each sub-basin reaches 0.01 to 10.32 m³/s.

The optimization measures of NH₃-N annual emissions based on water environmental capacity were proposed. By optimizing the annual emission intensity of NH₃-N, the

monthly average concentration of NH₃-N in the outlet section of the basin was significantly reduced (<1.99 mg/L), and it reached the water standard of Class V and above. In addition, the pollutant-holding capacity of rivers in summer and autumn could be effectively utilized, and that the water quality at the outlet of the river basin reaches the standard could be ensured by concentrating the discharge in July, August, and September.

Author Contributions: Data curation, L.C. and Y.L.; formal analysis, L.C.; funding acquisition, M.Y.; investigation, M.Y., Y.L. and L.N.; methodology, M.Y.; validation, Y.L.; writing—original draft, L.C.; writing—review and editing, L.C. All authors have read and agreed to the published version of the manuscript.

Funding: This research was funded by the Science and Technology Major Project for Water Pollution Control and Treatment (No. 2018ZX07111005), the National Science Foundation for Young Scientists of China (No. 51709271), and the Lift Program for Young Scientists of IWHR (SD0145B102021).

Institutional Review Board Statement: Not applicable.

Informed Consent Statement: Not applicable.

Data Availability Statement: Not applicable.

Conflicts of Interest: The authors declare no conflict of interest.

Appendix A

Table A1. Early warning value of upper limit of NH₃-N monthly emission in each sub-basin in different level years (t).

	SUB	Jan.	Feb.	Mar.	Apr.	May	Jun.	Jul.	Aug.	Sep.	Oct.	Nov.	Dec.
	1	1.20	1.08	0.76	3.34	1.96	0.43	18.23	10.21	6.87	3.92	2.38	1.02
	2	5.59	5.04	3.55	15.52	9.13	1.98	84.80	47.47	31.95	18.22	11.06	4.77
	3	1.42	1.28	0.90	3.93	2.31	0.50	21.49	12.03	8.10	4.62	2.80	1.21
	4	7.31	6.58	4.63	20.28	11.93	2.58	110.78	62.02	41.73	23.80	14.45	6.23
	5	0.00	0.00	0.00	0.00	0.00	0.00	0.01	0.01	0.00	0.00	0.00	0.00
	6	4.28	3.86	2.71	11.88	6.99	1.51	64.92	36.35	24.46	13.95	8.47	3.65
	7	10.52	9.48	6.67	29.18	17.16	3.72	159.41	89.24	60.06	34.24	20.79	8.96
	8	5.60	5.04	3.55	15.53	9.13	1.98	84.84	47.49	31.96	18.22	11.07	4.77
	9	1.44	1.30	0.91	3.99	2.35	0.51	21.80	12.21	8.21	4.68	2.84	1.23
	10	7.64	6.88	4.84	21.20	12.47	2.70	115.80	64.83	43.62	24.87	15.10	6.51
	11	19.34	17.42	12.26	53.66	31.56	6.84	293.12	164.10	110.43	62.97	38.23	16.48
	12	15.04	13.55	9.53	41.73	24.54	5.32	227.94	127.61	85.87	48.97	29.73	12.81
	13	11.06	9.96	7.01	30.68	18.05	3.91	167.60	93.83	63.14	36.00	21.86	9.42
	14	14.50	13.07	9.19	40.24	23.67	5.13	219.80	123.05	82.81	47.22	28.67	12.35
	15	1.81	1.63	1.15	5.01	2.95	0.64	27.39	15.33	10.32	5.88	3.57	1.54
	16	11.92	10.74	7.56	33.08	19.46	4.21	180.74	101.18	68.09	38.83	23.57	10.16
	17	20.32	18.31	12.88	56.39	33.17	7.18	308.05	172.46	116.06	66.17	40.18	17.31
High-flow years	18	5.47	4.93	3.47	15.19	8.93	1.93	82.96	46.44	31.25	17.82	10.82	4.66
	19	8.14	7.33	5.16	22.59	13.29	2.88	123.39	69.08	46.49	26.51	16.09	6.94
	20	9.25	8.34	5.86	25.67	15.10	3.27	140.24	78.51	52.83	30.13	18.29	7.88
	21	2.31	2.08	1.46	6.41	3.77	0.82	34.99	19.59	13.18	7.52	4.56	1.97
	22	5.56	5.01	3.53	15.44	9.08	1.97	84.33	47.21	31.77	18.12	11.00	4.74
	23	32.77	29.53	20.77	90.94	53.49	11.59	496.77	278.11	187.15	106.72	64.79	27.92
	24	2.26	2.04	1.43	6.28	3.70	0.80	34.32	19.21	12.93	7.37	4.48	1.93
	25	39.67	35.75	25.14	110.08	64.75	14.02	601.39	336.67	226.56	129.19	78.44	33.80
	26	1.34	1.21	0.85	3.73	2.19	0.48	20.37	11.41	7.68	4.38	2.66	1.15
	27	1.69	1.52	1.07	4.68	2.75	0.60	25.57	14.31	9.63	5.49	3.34	1.44
	28	6.60	5.94	4.18	18.30	10.76	2.33	99.97	55.97	37.66	21.48	13.04	5.62
	29	3.30	2.97	2.09	9.15	5.38	1.17	49.96	27.97	18.82	10.73	6.52	2.81
	30	15.25	13.74	9.66	42.31	24.89	5.39	231.16	129.41	87.09	49.66	30.15	12.99
	31	0.16	0.15	0.10	0.46	0.27	0.06	2.49	1.39	0.94	0.53	0.32	0.14
	32	36.90	33.25	23.39	102.39	60.22	13.04	559.33	313.13	210.72	120.15	72.95	31.44
	33	5.15	4.64	3.26	14.29	8.40	1.82	78.06	43.70	29.41	16.77	10.18	4.39
	34	5.31	4.78	3.36	14.72	8.66	1.88	80.42	45.02	30.30	17.28	10.49	4.52
	35	1.51	1.36	0.96	4.20	2.47	0.53	22.92	12.83	8.63	4.92	2.99	1.29

Table A1. Cont.

	SUB	Jan.	Feb.	Mar.	Apr.	May	Jun.	Jul.	Aug.	Sep.	Oct.	Nov.	Dec.	
Normal-flow years	1	1.18	1.14	1.15	1.44	3.79	0.52	9.44	15.29	13.09	4.99	2.16	0.85	
	2	5.48	5.28	5.33	6.69	17.61	2.40	43.91	71.14	60.86	23.20	10.06	3.95	
	3	1.39	1.34	1.35	1.70	4.46	0.61	11.13	18.03	15.42	5.88	2.55	1.00	
	4	7.16	6.90	6.96	8.74	23.01	3.14	57.37	92.93	79.51	30.30	13.14	5.16	
	5	0.00	0.00	0.00	0.00	0.00	0.00	0.00	0.01	0.01	0.01	0.00	0.00	0.00
	6	4.19	4.04	4.08	5.12	13.49	1.84	33.62	54.46	46.60	17.76	7.70	3.03	
	7	10.30	9.93	10.02	12.58	33.11	4.52	82.55	133.73	114.42	43.61	18.91	7.43	
	8	5.48	5.28	5.33	6.69	17.62	2.41	43.93	71.17	60.89	23.21	10.06	3.95	
	9	1.41	1.36	1.37	1.72	4.53	0.62	11.29	18.29	15.65	5.96	2.59	1.02	
	10	7.48	7.21	7.28	9.14	24.05	3.28	59.97	97.14	83.11	31.68	13.74	5.40	
	11	18.93	18.25	18.43	23.13	60.89	8.31	151.80	245.90	210.39	80.18	34.77	13.66	
	12	14.72	14.19	14.33	17.99	47.35	6.46	118.04	191.22	163.61	62.35	27.04	10.63	
	13	10.83	10.44	10.54	13.22	34.82	4.75	86.80	140.60	120.30	45.85	19.88	7.81	
	14	14.20	13.69	13.82	17.34	45.66	6.23	113.83	184.39	157.76	60.13	26.07	10.25	
	15	1.77	1.71	1.72	2.16	5.69	0.78	14.18	22.98	19.66	7.49	3.25	1.28	
	16	11.67	11.25	11.36	14.26	37.54	5.12	93.60	151.62	129.73	49.44	21.44	8.42	
	17	19.90	19.18	19.37	24.31	63.99	8.73	159.53	258.43	221.11	84.27	36.54	14.36	
	18	5.36	5.17	5.22	6.55	17.23	2.35	42.96	69.59	59.54	22.69	9.84	3.87	
	19	7.97	7.68	7.76	9.74	25.63	3.50	63.90	103.52	88.57	33.75	14.64	5.75	
	20	9.06	8.73	8.82	11.07	29.13	3.98	72.63	117.65	100.66	38.36	16.64	6.54	
	21	2.26	2.18	2.20	2.76	7.27	0.99	18.12	29.36	25.12	9.57	4.15	1.63	
	22	5.45	5.25	5.30	6.65	17.52	2.39	43.67	70.75	60.53	23.07	10.00	3.93	
	23	32.09	30.93	31.23	39.20	103.20	14.08	257.26	416.75	356.56	135.89	58.93	23.16	
	24	2.22	2.14	2.16	2.71	7.13	0.97	17.77	28.79	24.63	9.39	4.07	1.60	
	25	38.85	37.45	37.81	47.45	124.93	17.05	311.44	504.51	431.65	164.51	71.34	28.03	
	26	1.32	1.27	1.28	1.61	4.23	0.58	10.55	17.09	14.62	5.57	2.42	0.95	
	27	1.65	1.59	1.61	2.02	5.31	0.72	13.24	21.45	18.35	6.99	3.03	1.19	
	28	6.46	6.22	6.28	7.89	20.77	2.83	51.77	83.87	71.76	27.35	11.86	4.66	
	29	3.23	3.11	3.14	3.94	10.38	1.42	25.88	41.92	35.86	13.67	5.93	2.33	
	30	14.93	14.39	14.53	18.24	48.02	6.55	119.71	193.92	165.91	63.23	27.42	10.77	
	31	0.16	0.15	0.16	0.20	0.52	0.07	1.29	2.09	1.79	0.68	0.30	0.12	
	32	36.13	34.83	35.16	44.13	116.19	15.86	289.66	469.22	401.46	153.01	66.35	26.07	
	33	5.04	4.86	4.91	6.16	16.21	2.21	40.42	65.48	56.03	21.35	9.26	3.64	
	34	5.19	5.01	5.06	6.35	16.71	2.28	41.65	67.47	57.72	22.00	9.54	3.75	
	35	1.48	1.43	1.44	1.81	4.76	0.65	11.87	19.23	16.45	6.27	2.72	1.07	
Low-flow years	1	1.70	1.79	0.50	1.52	1.49	1.51	18.96	13.32	11.53	3.99	0.55	1.50	
	2	7.91	8.34	2.35	7.08	6.95	7.01	88.19	61.94	53.63	18.54	2.56	6.98	
	3	2.01	2.11	0.60	1.79	1.76	1.78	22.35	15.70	13.59	4.70	0.65	1.77	
	4	10.34	10.89	3.07	9.25	9.08	9.16	115.21	80.91	70.07	24.23	3.34	9.12	
	5	0.00	0.00	0.00	0.00	0.00	0.00	0.01	0.01	0.01	0.00	0.00	0.00	
	6	6.06	6.38	1.80	5.42	5.32	5.37	67.52	47.42	41.06	14.20	1.96	5.34	
	7	14.88	15.67	4.41	13.31	13.07	13.19	165.79	116.43	100.83	34.86	4.81	13.12	
	8	7.92	8.34	2.35	7.08	6.95	7.02	88.23	61.97	53.66	18.55	2.56	6.98	
	9	2.04	2.14	0.60	1.82	1.79	1.80	22.68	15.93	13.79	4.77	0.66	1.79	
	10	10.81	11.38	3.21	9.67	9.49	9.58	120.43	84.58	73.24	25.32	3.49	9.53	
	11	27.36	28.81	8.12	24.47	24.02	24.25	304.85	214.10	185.40	64.11	8.85	24.12	
	12	21.28	22.41	6.31	19.03	18.68	18.85	237.06	166.49	144.17	49.85	6.88	18.76	
	13	15.64	16.47	4.64	13.99	13.74	13.86	174.31	122.42	106.01	36.65	5.06	13.79	
	14	20.52	21.61	6.09	18.35	18.02	18.18	228.60	160.54	139.03	48.07	6.63	18.09	
	15	2.56	2.69	0.76	2.29	2.24	2.27	28.49	20.01	17.32	5.99	0.83	2.25	
	16	16.87	17.77	5.00	15.09	14.81	14.95	187.97	132.01	114.32	39.53	5.46	14.87	
	17	28.75	30.28	8.53	25.71	25.25	25.48	320.38	225.00	194.85	67.37	9.30	25.35	
	18	7.74	8.15	2.30	6.92	6.80	6.86	86.28	60.59	52.47	18.14	2.50	6.83	
	19	11.52	12.13	3.42	10.30	10.11	10.21	128.33	90.13	78.05	26.99	3.72	10.15	
	20	13.09	13.79	3.88	11.71	11.49	11.60	145.85	102.43	88.70	30.67	4.23	11.54	
	21	3.27	3.44	0.97	2.92	2.87	2.89	36.39	25.56	22.13	7.65	1.06	2.88	
	22	7.87	8.29	2.34	7.04	6.91	6.98	87.71	61.60	53.34	18.44	2.55	6.94	
	23	46.37	48.83	13.76	41.47	40.72	41.09	516.65	362.84	314.21	108.64	14.99	40.88	
	24	3.20	3.37	0.95	2.86	2.81	2.84	35.69	25.07	21.71	7.51	1.04	2.82	
	25	56.13	59.11	16.65	50.20	49.29	49.74	625.45	439.25	380.38	131.52	18.15	49.49	
	26	1.90	2.00	0.56	1.70	1.67	1.69	21.19	14.88	12.89	4.46	0.61	1.68	
	27	2.39	2.51	0.71	2.13	2.10	2.12	26.59	18.68	16.17	5.59	0.77	2.10	
	28	9.33	9.83	2.77	8.34	8.19	8.27	103.97	73.02	63.23	21.86	3.02	8.23	
	29	4.66	4.91	1.38	4.17	4.10	4.13	51.96	36.49	31.60	10.93	1.51	4.11	
	30	21.58	22.72	6.40	19.30	18.95	19.12	240.41	168.84	146.21	50.55	6.98	19.02	
	31	0.23	0.24	0.07	0.21	0.20	0.21	2.59	1.82	1.57	0.54	0.08	0.20	
	32	52.21	54.98	15.49	46.69	45.84	46.27	581.70	408.53	353.78	122.32	16.88	46.02	
	33	7.29	7.67	2.16	6.52	6.40	6.46	81.18	57.01	49.37	17.07	2.36	6.42	
	34	7.51	7.91	2.23	6.71	6.59	6.65	83.64	58.74	50.87	17.59	2.43	6.62	
	35	2.14	2.25	0.63	1.91	1.88	1.90	23.84	16.74	14.50	5.01	0.69	1.89	

References

- Sun, T.; Cheng, W.Q.; Bo, Q.Y.; Meng, X.; Liang, D. Analysis on historical flood and countermeasures in prevention and control of flood in Daqing River Basin. *Environ. Res.* **2021**, *196*, 110895.
- Li, S.C.; Zhao, Y.L.; Xiao, W.; Yue, W.Z.; Wu, T. Optimizing ecological security pattern in the coal resource-based city: A case study in Shuozhou City, China. *Ecol. Indic.* **2021**, *130*, 108026. [[CrossRef](#)]
- Chanapathi, T.; Thatikonda, S. Fuzzy-based regional water quality index for surface water quality assessment. *J. Hazard. Toxic Radioact. Waste* **2019**, *23*, 04019010. [[CrossRef](#)]
- Kachroud, M.; Trolard, F.; Kefi, M.; Jaber, S.; Bourrié, G. Water quality indices: Challenges and application limits in the literature. *Water* **2019**, *11*, 361. [[CrossRef](#)]
- Najafzadeh, M.; Homaei, F.; Farhadi, H. Reliability assessment of water quality index based on guidelines of national sanitation foundation in natural streams: Integration of remote sensing and data-driven models. *Artif. Intell. Rev.* **2021**, *54*, 4619–4651. [[CrossRef](#)]
- Najafzadeh, M.; Niazmardi, S. A Novel Multiple-Kernel Support Vector Regression Algorithm for Estimation of Water Quality Parameters. *Nat. Resour. Res.* **2021**, *30*, 3761–3775. [[CrossRef](#)]
- Jamei, M.; Ahmadianfar, I.; Chu, X.; Yaseen, Z.M. Prediction of surface water total dissolved solids using hybridized wavelet-multigene genetic programming: New approach. *J. Hydrol.* **2020**, *589*, 125335. [[CrossRef](#)]
- Najafzadeh, M.; Ghaemi, A. Prediction of the five-day biochemical oxygen demand and chemical oxygen demand in natural streams using machine learning methods. *Environ. Monit. Assess.* **2019**, *191*, 380. [[CrossRef](#)]
- Najafzadeh, M.; Ghaemi, A.; Emamgholizadeh, S. Prediction of water quality parameters using evolutionary computing-based formulations. *Int. J. Environ. Sci. Technol.* **2018**, *16*, 6377–6396. [[CrossRef](#)]
- Lee, J.; Chae, K.J. A systematic protocol of microplastics analysis from their identification to quantification in water environment: A comprehensive review. *J. Hazard. Water* **2020**, *403*, 124049. [[CrossRef](#)]
- Gumbo, A.D.; Kapangaziwiri, E.; Chikoore, H.; Pienaar, H.; Mathivha, F. Assessing water resources availability in headwater sub-catchments of Pungwe River Basin in a changing climate. *J. Hydrol.* **2021**, *35*, 100827. [[CrossRef](#)]
- Korytny, L.M. The basin concept: From hydrology to nature management. *Geogr. Nat. Resour.* **2017**, *38*, 111–121. [[CrossRef](#)]
- Tsihrintzis, V.A.; Vangelis, H. Water Resources and Environment. *Water Resour. Manag.* **2018**, *32*, 4813–4817. [[CrossRef](#)]
- Zhou, X.Y.; Wang, F.; Huang, K.; Zhang, H.C.; Yu, J.; Alan, Y.H. System Dynamics-Multiple Objective Optimization Model for Water Resource Management: A Case Study in Jiaying City, China. *Water* **2021**, *13*, 671. [[CrossRef](#)]
- Georgakakos, A.P.; Marks, D.H. A new method for the real-time operation of reservoir systems. *Water Resour. Res.* **1987**, *23*, 1376–1390. [[CrossRef](#)]
- Brmus, N. *Scientific Allocation of Water Resources*; Water Conservancy and Electric Power Press: Beijing, China, 1983.
- Apaydin, H.; Feizi, H.; Sattari, M.T.; Colak, M.S.; Shamshirband, S.; Chau, K.W. Comparative Analysis of Recurrent Neural Network Architectures for Reservoir Inflow Forecasting. *Water* **2020**, *12*, 1500. [[CrossRef](#)]
- Thuc, D.P.; Edoardo, B.; Rodney, A.S. Critical review of system dynamics modelling applications for water resources planning and management. *Clean. Environ. Syst.* **2021**, *2*, 100031.
- Obeysekera, J.; Barnes, J.; Nungesser, M. Climate Sensitivity Runs and Regional Hydrologic Modeling for Predicting the Response of the Greater Florida Everglades Ecosystem to Climate Change. *Environ. Manag.* **2015**, *55*, 749–762. [[CrossRef](#)]
- Zhang, Q.; Liu, J.; Singh, V.P.; Shi, P.; Sun, P. Hydrological responses to climatic changes in the Yellow River basin, China: Climatic elasticity and streamflow prediction. *J. Hydrol.* **2017**, *554*, 635–645. [[CrossRef](#)]
- Singh, V.P. Hydrologic modeling: Progress and future directions. *Geosci. Lett.* **2018**, *5*, 15–33. [[CrossRef](#)]
- Gholizadeh, M.; Nabizadeh, E.; Mahamadpur, O. Optimization of water quantity and quality in Mahabad River by SWAT model. *Res. Mar. Sci.* **2017**, *2*, 112–129.
- Abdulkareem, J.H.; Pradhan, B.; Sulaiman, W.N.A.; Jamil, N.R. Review of studies on hydrological modelling in Malaysia. *Model. Earth Syst. Environ.* **2018**, *4*, 1577–1605. [[CrossRef](#)]
- Ma, C.K.; Sun, L.; Liu, S.Y.; Shao, M.A.; Luo, Y. Impact of climate change on the streamflow in the glacierized Chu River Basin, Central Asia. *J. Arid Land* **2015**, *7*, 501–513. [[CrossRef](#)]
- Tang, X.P.; Zhang, J.Y.; Wang, G.Q.; Jin, J.L.; Liu, C.S.; Liu, Y.L.; He, R.M.; Bao, Z.X. Uncertainty Analysis of SWAT Modeling in the Lancang River Basin Using Four Different Algorithms. *Water* **2021**, *13*, 341. [[CrossRef](#)]
- Mousavi, R.; Ahmadzadeh, M.; Marofi, S. A Multi-GCM Assessment of the Climate Change Impact on the Hydrology and Hydropower Potential of a Semi-Arid Basin (A Case Study of the Dez Dam Basin, Iran). *Water* **2018**, *10*, 1458. [[CrossRef](#)]
- Mao, F.; Shen, Z.Y. Assessment of the Impacts of Land Use Change on Non-Point Source Loading under Future Climate Scenarios Using the SWAT Model. *Water* **2021**, *13*, 874.
- Franciane, M.D.S.; Rodrigo, P.D.O.; Frederico, F.M. Evaluating a parsimonious watershed model versus SWAT to estimate streamflow, soil loss and river contamination in two case studies in Tietê river basin, São Paulo, Brazil. *J. Hydrol.* **2020**, *29*, 100685.
- Das, B.; Singh, A.; Panda, S.N.; Yasuda, H. Optimal land and water resources allocation policies for sustainable irrigated agriculture. *Land Use Policy* **2015**, *42*, 527–537. [[CrossRef](#)]
- Zarghami, M.; Safari, N.; Szidarovszky, F.; Islam, S. Nonlinear Interval Parameter Programming Combined with Cooperative Games: A Tool for Addressing Uncertainty in Water Allocation Using Water Diplomacy Framework. *Water Resour. Manag.* **2015**, *29*, 4285–4303. [[CrossRef](#)]

31. Nematian, J. An Extended Two-stage Stochastic Programming Approach for Water Resources Management under Uncertainty. *J. Environ. Inform.* **2016**, *27*, 72–84. [[CrossRef](#)]
32. Perciac, O.M. Optimal operation of regional system with diverse water quality sources. *J. Water Res. Plan. Manag.* **1997**, *123*, 105–115. [[CrossRef](#)]
33. Gassman, P.W.; Reyes, M.R.; Green, C.H.; Arnold, J.G. The Soil and Water Assessment Tool: Historical Development, Applications, and Future Research Directions. *Trans. ASABE* **2007**, *50*, 1211–1250. [[CrossRef](#)]
34. Pourmand, E.; Mahjouri, N. A fuzzy multi-stakeholder multi-criteria methodology for water allocation and reuse in metropolitan areas. *Environ. Monit. Assess.* **2018**, *190*, 444. [[CrossRef](#)] [[PubMed](#)]
35. Yu, S.; He, L.; Lu, H.W. An environmental fairness-based optimisation model for the decision-support of joint control over the water quantity and quality of a river basin. *J. Hydrol.* **2016**, *535*, 366–376. [[CrossRef](#)]
36. Kahil, M.T.; Dinar, A.; Albiac, J. Cooperative water management and ecosystem protection under scarcity and drought in arid and semiarid regions. *Water Resour. Econ.* **2016**, *13*, 60–74. [[CrossRef](#)]
37. Xu, G.; Feng, M. Joint risk of water quantity and quality in water sources of water diversion project. *J. Northwest. A F Univ. (Nat. Sci. Ed.)* **2016**, *44*, 228–234.
38. Zegpi, M.; Fernandez, B. Hydrological model for urban catchments—analytical development using copulas and numerical solution. *Hydrol. Sci. J.* **2010**, *55*, 1123–1136. [[CrossRef](#)]
39. Guo, A.; Chang, J.; Wang, Y.; Li, Y. Variation characteristics of rainfall-runoff relationship and driving factors analysis in Jinghe River Basin in nearly 50 years. *Trans. Chin. Soc. Agric. Eng.* **2015**, *31*, 165–171.
40. Lv, J.; Shen, B.; Li, H.; Jiang, Y. Study on the runoff response to climate change—a case study of source region of the Yellow River. *J. Hydroelectr. Eng.* **2015**, *34*, 191198.
41. Li, F.; Zheng, Q. Probabilistic modelling of flood events using the entropy copula. *Adv. Water Resour.* **2016**, *97*, 233–240. [[CrossRef](#)]
42. Debele, S.E.; Bogdanowicz, E.; Strupczewski, W.G. The impact of seasonal flood peak dependence on annual maxima design quantiles. *Hydrol. Sci. J.* **2017**, *62*, 1603–1617. [[CrossRef](#)]
43. Yang, R.; Wu, S.Q.; Gao, X.P.; Zhang, C. A vine copula-based study on identification of multivariate water environmental risk under different connectivity of rivers and lakes. *J. Hydraul. Eng.* **2020**, *51*, 606–616.
44. Yu, R.; Yang, R.; Zhang, C.; Špoljar, M.; Kuczyńska-Kippen, N.; Sang, G. A Vine Copula-based modeling for identification of multivariate water pollution risk in an Interconnected River System Network. *Water* **2020**, *12*, 2741. [[CrossRef](#)]
45. Yu, R.; Zhang, C. Early warning of water quality degradation: A copula-based bayesian network model for highly efficient water quality risk assessment. *J. Environ. Manag.* **2021**, *292*, 112749. [[CrossRef](#)]
46. Arya, F.K.; Zhang, L. Copula-based Markov process for forecasting and analyzing risk of water quality time series. *J. Hydrol. Eng.* **2017**, *22*, 04017005. [[CrossRef](#)]
47. Qin, Y.; Elizabeth, C.; Grant, M.K.; Julian, M.A.; Keith, S.R. China’s energy-water nexus—Assessment of the energy sector’s compliance with the “3 Red Lines” industrial water policy Energy Policy. *Energy Policy* **2015**, *82*, 131–143. [[CrossRef](#)]
48. Chao, H.P.; Lee, J.F.; Cary, T.C. Corrigendum to “Determination of the Henry’s law constants of low volatility compounds via the measured air-phase transfer coeffic. *Water Res.* **2017**, *120*, 238–244. [[CrossRef](#)]
49. Choi, J.R.; Chung, I.M.; Jeung, S.J.; Choo, K.S.; Oh, C.H.; Kim, B.S. Development and Verification of the Available Number of Water Intake Days in Ungauged Local Water Source Using the SWAT Model and Flow Recession Curves. *Water* **2021**, *13*, 1511. [[CrossRef](#)]
50. Hoshin, V.G.; Harald, K.; Koray, K.Y.; Guillermo, F.M. Decomposition of the mean squared error and NSE performance criteria: Implications for improving hydrological modelling. *J. Hydrol.* **2009**, *377*, 80–91.
51. Moriasi, D.N.; Arnold, J.G.; Liew, M.W.V.; Bingner, R.L.; Harmel, R.D.; Veith, T.L. Model Evaluation Guidelines for Systematic Quantification of Accuracy in Watershed Simulations. *Trans. ASABE* **2007**, *50*, 885–900. [[CrossRef](#)]
52. Suresh, M.; Laxmi, P.D.; Deepak, A. Application of SWAT in Hydrological Simulation of Complex Mountainous River Basin (Part I: Model Development). *Water* **2021**, *13*, 1546.
53. Gao, Y.Q.; Yuan, Y.; Wang, H.Z.; Zhang, Z.X.; Ye, L. Analysis of impacts of polders on flood processes in Qinghai River Basin, China, using the HEC-RAS model. *Water Sci. Technol.-Water Supply* **2018**, *18*, 1852–1860. [[CrossRef](#)]
54. Conant, B., Jr.; Robinson, C.E.; Hinton, M.J.; Russell, H.A.J. A framework for conceptualizing groundwater-surface water interactions and identifying potential impacts on water quality, water quantity, and ecosystems. *J. Hydrol.* **2019**, *574*, 609–627. [[CrossRef](#)]
55. Li, W.H.; Zhou, Y.D.; Deng, Z.J. The Effectiveness of “River Chief System” Policy: An Empirical Study Based on Environmental Monitoring Samples of China. *Water* **2021**, *13*, 1988. [[CrossRef](#)]
56. Gong, Y.X.; Ji, X.; Hong, X.C.; Cheng, S.S. Correlation Analysis of Landscape Structure and Water Quality in Suzhou National Wetland Park, China. *Water* **2021**, *13*, 2075. [[CrossRef](#)]
57. Huang, J.C.; Zhang, Y.J.; Bing, H.J.; Peng, J.; Dong, F.F.; Gao, J.F.; George, B.A. Characterizing the river water quality in China: Recent progress and on-going challenges. *Water Res.* **2021**, *201*, 117309. [[CrossRef](#)]
58. Megan, S.; John, R.; Kevin, M.; Rachael, S.; Robin, E.; David, W.; Jane, W. Targeting for pollutant reductions in the Great Barrier Reef River catchments. *Environ. Sci. Policy* **2018**, *89*, 365–377.
59. Li, P.; Xu, G.C.; Lu, K.X. Runoff change and sediment source during rainstorms in an ecologically constructed watershed on the Loess Plateau, China. *Sci. Total Environ.* **2019**, *664*, 968–974. [[CrossRef](#)]